STUDIES ON THE INJECTION EFFICIENCY IN THE ESR

A. Sherjan*[1,2], G. Franchetti[1,2,3]
[1]GSI Helmholtz Centre for Heavy Ion Research, Darmstadt, Germany
[2]Goethe University Frankfurt, Frankfurt am Main, Germany
[3]HFHF Helmholtz Research Academy Hesse for FAIR, Frankfurt am Main, Germany

Abstract

The ESR (Experimental Storage Ring) at GSI is one of the very few facilities that can offer highly charged heavy ion beams for precise atomic physics experiments. With each experiment during the beam time the requirements on the storage ring are changing and so the machine needs to be prepared every time from the beam injection to the extraction accordingly. In order to find the optimal setting for the injection it can practically mean to scan from scratch over several parameters, which can vary for different machine settings and therefore it can become time consuming. We present in this proceeding a general analysis on the beam transmission at injection depending on the injection machine parameters and beam properties supported by simulations and tests. Based on this study, we propose a fast method to find the optimal parameter settings, especially in case of partially unknown properties.

MOTIVATION

During the Machine Development 2025 at the ESR, among other measurements [1, 2], there was a first attempt to measure the resonance chart of this storage ring [3]. To achieve this, the beam needs to be injected at different working points of the machine. Then the tune needs to be moved across the tune diagram along established lines while storing the beam intensity. This allows detecting beam losses due to resonance crossing [4]. At the ESR, the application of this procedure has encountered an unexpected difficulty. The tune scan could not be carried out as there were only two stable working points at which the beam could be injected, any other working point caused an immediate beam loss even before changing the tune. Because of this difficulty we here investigate the process of injection in the ESR to obtain a scheme for the injection, which combines all the relevant parameters and their impact on the transmission efficiency. Ultimately, we aim to propose a fast approach for determining optimal injection parameters for any machine setting to resolve the issues in the measurements on the resonance chart.

CHALLENGE

The injection process in the ESR is a single turn injection. The incoming beam receives a first deflection by the septum magnet to adjust the beam angle right at injection [5] and a second kick by a fast kicker to reduce the betatron oscillations of the beam before it reaches the septum again, see Fig. 1, [6]. The main parameters with an impact on the injection efficiency regarding the beam are: the beam size, x_E; the position and the angle of the beam centroid at injection, (x_0, x_0'). The relevant machine parameters for the process are: the transverse position of the magnetic septum, x_S, and the deflecting angle exerted by the septum, θ_S (see Fig. 1); the injection kicker correction angle, θ_K; the tune of the machine, Q_x, that defines the phase advance $\Delta\psi$ between the septum and the kicker; the closed orbit (CO) distortion, (x_{co}, x_{co}') at the septum. Unfortunately at the ESR the sequence of beam position monitors available does not allow to retrieve the CO at the injection septum, although they clearly show the presence of CO deformations. Additionally, the information on the beam at injection are also not precisely known, hence, the challenge is to find an optimization procedure which is effective in spite of these unknown.

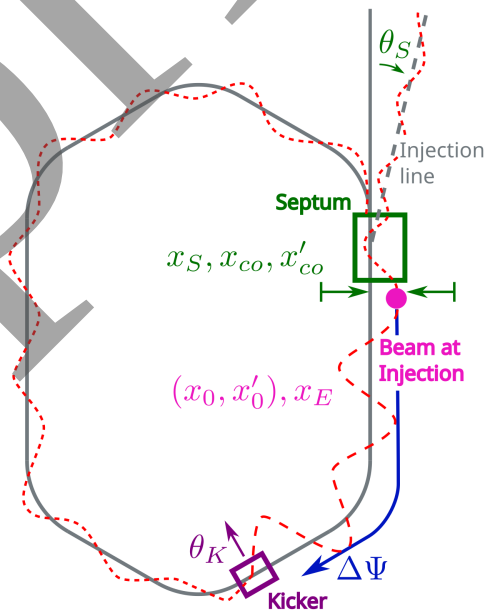

Figure 1: Schematic view of relevant parameters at injection.

METHODOLOGY

As shown in previous studies [7–10], instead of using the lab frame (x, x'), it is more convenient to describe the process of one-turn injection in the Courant-Snyder (CS) reference frame, $(\hat{x}, \hat{x}')$. See Fig. 2 for reference. The benefit of this choice is that the beam motion becomes a rigid rotation around the CO. As the CO is also changing along the ring, the total motion of the beam becomes a superposition of both, the change of the CO itself and the rotation around it. Therefore it is convenient to describe the dynamics with re-

* a.sherjan@gsi.de

spect to the CO, here expressed with the coordinates $(\tilde{x}, \tilde{x}')$, see Fig. 2. The dynamics of the beam from the injection location after the deflection septum, $(\tilde{x}_0, \tilde{x}'_0 + \tilde{\theta}_S)$, to the injection kicker location, $(\tilde{x}_1, \tilde{x}'_1)$, is given by a single rotation by $\Delta\psi$ around $(\hat{x}_{co}, \hat{x}'_{co})$. The initial deflection by the septum magnet, $\tilde{\theta}_s$, the transport, and afterwards the kick by the injection kicker, $\tilde{\theta}_K$, results in a shift of the beam's phase space position to $(\tilde{x}_2, \tilde{x}'_2)$. In the real machine, once the tune

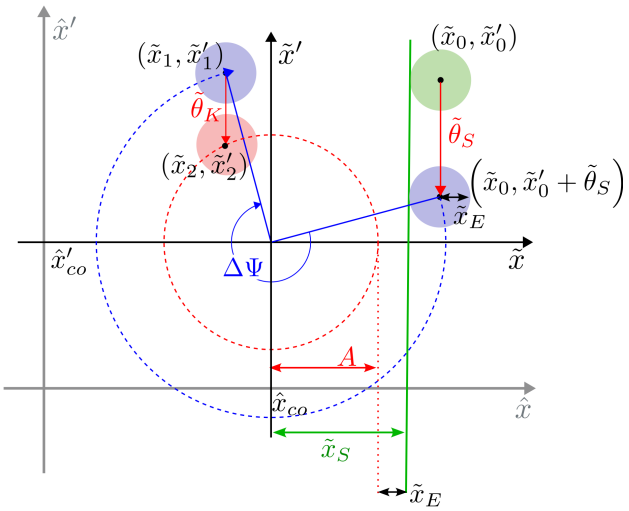

Figure 2: Schematic view of the one-turn injection dynamics in the Courant-Snyder coordinates.

has been set, the two angles, $\tilde{\theta}_S$ and $\tilde{\theta}_K$, can be chosen freely within the technical limitations to optimize the beam transmission at injection. For an efficient injection, however, the kick applied by the injection kicker needs to shift the beam centroid closer to the CO, in order to reduce the amplitude of oscillations A less or equal to $|\tilde{x}_S - \tilde{x}_E|$, otherwise the beam is eventually scraped at the septum, see Fig. 2. Here $\tilde{x}_E$ is the beam size. It is straightforward to compute the values of $\tilde{\theta}_S$ and $\tilde{\theta}_K$ satisfying the "edge condition" $A = |\tilde{x}_S - \tilde{x}_E|$ as

$$\begin{aligned} 0 &= \tilde{\theta}_S^2 + 2\,\cos\psi\,\tilde{\theta}_S\,\tilde{\theta}_K + \tilde{\theta}_K^2 \\ &+ 2\,\tilde{x}'_0\,\tilde{\theta}_S + (2\,\cos\psi\,\tilde{x}'_0 - 2\,\sin\psi\,\tilde{x}_0)\,\tilde{\theta}_K \\ &- (\tilde{x}_S - \hat{x}_E)^2 + (\tilde{x}_0^2 + \tilde{x}_0'^2)\;; \end{aligned} \tag{1}$$

this equation describes an ellipse in the $(\tilde{\theta}_S, \tilde{\theta}_K)$ space. All values of $\tilde{\theta}_S, \tilde{\theta}_K$ inside this ellipse will guarantee full beam transmission.

SIMULATIONS

For the systematic studies on the beam transmission, the 2D-parameter space $(\tilde{\theta}_S, \tilde{\theta}_K)$ was scanned in beam transport simulations for different scenarios and settings. Figure 3 displays a simulation example for an injected KV-beam, with the simulation settings listed in Table 1. The Fig. 3 top-left shows that the transmission plotted over the 2D-parameters scan is a continuous function, which forms an ellipsoidal shape. This picture also depicts with a dashed line the ellipse given by the "edge" condition Eq. 1, which is visibly consistent with the simulation results. The ellipsoidal shape of the

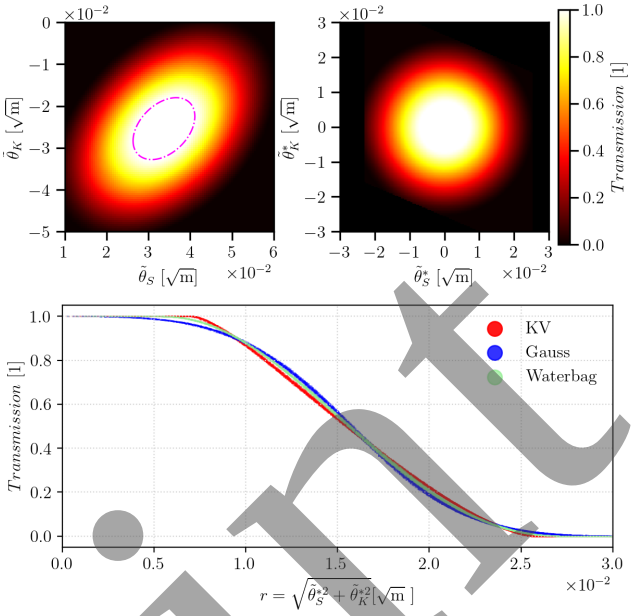

Figure 3: Top-left shows the transmission efficiency as function of $(\tilde{\theta}_S, \tilde{\theta}_K)$. The dashed ellipse shows the analytical solution for the "edge" transmission in comparison. Top-right shows the transmission as function of $(\tilde{\theta}^*_S, \tilde{\theta}^*_K)$ once normalized. The bottom shows how well is the transmission related to radius r, hence defining a general function characterizing the injection efficiency.

Table 1: Simulation Settings as one Representative Scenario Used for the Results of Fig. 3

Setting	Value	Unit
$E_{x,rms}$	20	mm-mrad
Npar	10^4	1
Turns	110	1
Q_x, Qy	2.425 , 2.223	1
x_{sep}	70	mm
x_{co}	-12.93	mm
x'_{co}	-1.03 $\times 10^{-1}$	mrad
$\Delta\psi$	0.69 $\times 2\pi$	1

transmission function, which results directly from the simulations, is then transformed to new coordinates $(\tilde{\theta}^*_S, \tilde{\theta}^*_K)$, via a Courant-Snyder-type of mapping, which is area preserving and normalizes ellipses into circles. Within the scope of this paper, the transformation rules cannot be discussed in detail, we rather focus on the implication of using this approach. In the coordinates $(\tilde{\theta}^*_S, \tilde{\theta}^*_K)$, the circular symmetry is restored as shown in Fig. 3 top-right, and this allows to describe the transmission with only one parameter by introducing the radius, $r = \sqrt{\tilde{\theta}^{*2}_S + \tilde{\theta}^{*2}_K}$. By plotting the transmission over this radius we can obtain a characteristic curve which describes the injection efficiency. This is shown in the Fig. 3 bottom for different type of injected beam distributions. Note that this procedure allows to characterize the injection efficiency

with a single curve. This finding is applicable for different scenarios and allows to derive a strategy of optimization.

Dispersion and Chromaticity

Next, we present additional simulation test cases in which the effects of the dispersion and the chromaticity are investigated separately to put the robustness of the derived model from Fig. 3 to the test. Figure 3 shows that it is enough to confine the following investigations to one type of beam, for example here we choose the KV distribution. For each of the effects, dispersion (Fig. 4) and chromaticity (Fig. 5), two scenarios were tested: The first example, Fig. 4 left and Fig. 5 left, shows the transmission for a beam with a coherent momentum offset, δ, and a momentum spread, Δ, for some roughly representative values from the real machine. The second example, Fig. 4 right and Fig. 5 right shows the transmission for a beam without a coherent momentum offset, but with increased momentum spread Δ, to test more extreme cases. Including the dispersion, the transmission curve at the region of the slope results in an overall broadening, see Fig. 4. Instead of a well-defined curve as in Fig. 3, it now broadens rather asymmetrically. Also the chromaticity causes a general spread of the transmission curve along the slope, which in this case seems to be more symmetrical, see Fig. 5. Even including the impact of dispersion

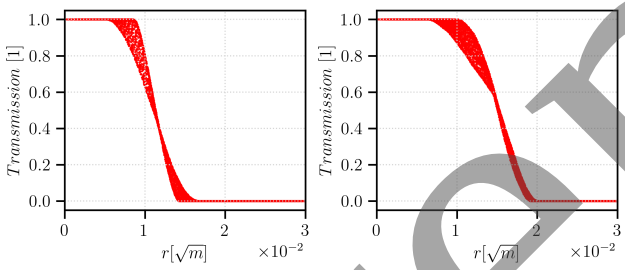

Figure 4: Including Dispersion. Left) KV-Beam with a coherent momentum offset $\delta = 1\%$ and a momentum spread of $\Delta = \pm 0.25\%$. Right) KV-Beam with $\delta = 0\%$ and $\Delta = \pm 0.6\%$.

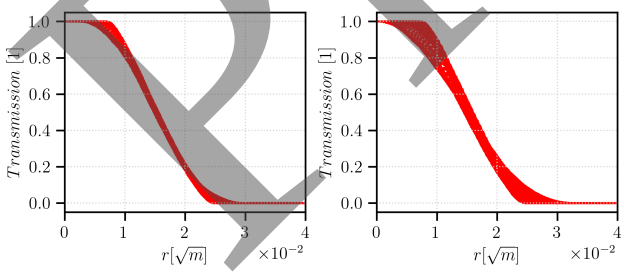

Figure 5: Including Chromaticity. Left) KV-Beam with a coherent momentum offset by $\delta = 1\%$ and a momentum spread of $\Delta = \pm 2.5\%$. Right) a KV-Beam with $\delta = 0\%$ and $\Delta = \pm 4\%$.

and chromaticity in the dynamics, the transmission curve, which models the injection efficiency, still provides the general trend of a continuously increasing function towards a preferable setting for maximum beam transmission.

OPTIMIZATION METHOD

These findings allow to devise a method for optimizing single-turn-injection in spite of the lack of knowledge of some parameters. The method, that can be used practically to optimize the injection efficiency, is next demonstrated with a simulation representing a measurement scenario in a real machine. First step is to set a randomly chosen pair of values, $\tilde{\theta}_S, \tilde{\theta}_K$ with a transmission > 0, see P1 in Table 2. From there two other measurement points (P2, P3) are needed: for example by keeping one parameter constant and changing the other and vice versa. With the transmission in P1, P2 and P3, we can determine the gradient of the transmission function in order to set the direction of the optimum for changing $\tilde{\theta}_S, \tilde{\theta}_K$: This is guaranteed by previous findings, which are also shown in Fig. 6. With a first order linear approximation also the optimal values for $\tilde{\theta}_S, \tilde{\theta}_K$ can be estimated.

Table 2: Simulated Measurement Used for the Demonstration of the Proposed Optimization Method in Fig. 2

Point	$\tilde{\theta}_S$	$\tilde{\theta}_K$	**Transmission**
P1	0.021	- 0.02	0.315
P2	0.017	-0.02	0.107
P3	0.021	-0.03	0.797

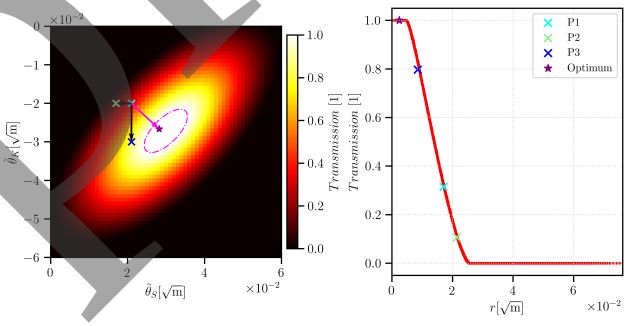

Figure 6: Example of the optimization procedure for the injection efficiency. The magenta arrow is the direction of optimization.

CONCLUSION

Simulations have shown that the beam transmission as a 2D parameter scan of the septum deflection angle and the injection kicker angle results in a continuous function. With suitable transformation rules the transmission function becomes a characteristic curve as a measure for the injection efficiency. The approach was tested for different beam distributions and including the effect of dispersion and chromaticity. From these simulation follows a quick method to optimize the injection parameters for this type of single turn injection schemes.

REFERENCES

[1] A. Heinz, G. Franchetti, A. Sherjan, J. Rausch and B. Lorentz, "Beam based optimization of the ESR linear optics model"

in Proc. IPAC'26, Deauville, France, 2026, paper WEP5015, to be published

[2] J. Rausch, A. Sherjan, G. Franchetti and B. Lorentz, "Retrieving the longitudinal nonlinear tunes from FCT measurements" in Proc. IPAC'26, Deauville, France, 2026, paper THP4079, to be published

[3] A. Sherjan, G. Franchetti and J. Rausch, "Experimental Resonance studies at the ESR" in Proc. IPAC'26, Deauville, France, 2026, paper THP4075, to be published

[4] G. Franchetti *et al.*, "Experiment on space charge driven nonlinear resonance crossing in an ion synchrotron", *Phys. Rev. Spec. Top. Accel. Beams*, vol. 13, no. 11, p. 114203, Nov. 2010. doi:10.1103/PhysRevSTAB.13.114203

[5] P. Spiller, W. Bourgeois, A. Dolinsky, H. Eickhoff, B. Frantzke, "Optimization of the Injection Optics of the Experimental Storage Ring", GSI Scientific Report 1996, p. 165.

[6] B. Franzke, "The Heavy Ion Storage and Cooler Ring Project ESR at GSI", *Nucl. Instrum. Methods Phys. Res. B*, vol. 24–25, pp. 18–25, 1987. doi:10.1016/0168-583X(87)90583-0

[7] B. Goddard, "Injection and extraction", CERN Accelerator School: Introduction to Accelerator Physics, Divonne-les-Bains, France, Feb. 23–27, 2009. https://cas.web.cern.ch/sites/default/files/lectures/divonne-2009/goddardpdf.pdf

[8] M. Plum and U. Wienands, "Injection and extraction, single turn injection", USPAS: Injection and Extraction, lecture notes, 2009. https://web.ornl.gov/~plumma/Plum_3_single_turn_inj.pdf

[9] Y. Kobayashi and K. Harada, "Possibility of the Beam Injection Using a Single Pulsed Sextupole Magnet in Electron Storage Rings" in *Proc. EPAC'06*, Edinburgh, Scotland, 2006, paper THPLS107. https://proceedings.jacow.org/e06/PAPERS/THPLS107.pdf

[10] F. Tecker, "Injection and Extraction", Proceedings of the CERN Accelerator School, 2021. doi:10.48550/arXiv.2108.11160